Automotive Innovation (2019) 2:79–92
https://doi.org/10.1007/s42154-019-00056-2

A Review of Engine Fuel Injection Studies Using Synchrotron Radiation X-ray Imaging

Zhijun Wu[1] · Wenbo Zhao[1] · Zhilong Li[1] · Jun Deng[1] · Zongjie Hu[1] · Liguang Li[1]

Received: 31 January 2019 / Accepted: 15 April 2019 / Published online: 21 May 2019

Abstract
Fuel spray characteristics directly determine the formation pattern and quality of the fuel/air mixture in an engine, and thus affect the combustion process. For this reason, the improvement and optimization of fuel injection systems is crucial to the development of engine technologies. The fuel jet breakup and atomization process is a complex liquid–gas two-phase turbulent flow system that has not yet been fully elucidated. Owing to the limitations of standard optical measurement techniques, the spray breakup mechanism and its interaction with the nozzle internal flow are still unclear. However, in recent years synchrotron radiation (SR) X-ray imaging technologies have been widely applied in engine fuel injection studies because of the higher energy and brilliance of third-generation SR light sources. This review provides a brief introduction to the development of SR technology and compares the critical parameters of the primary third-generation SR light sources available worldwide. The basic principles and applications of various X-ray imaging technologies with regard to nozzle internal structure measurements, visualization of in-nozzle flow characteristics and quantitative analyses of near-field spray transient dynamics are examined in detail.

Keywords X-ray imaging technology · Fuel injection · Nozzle internal structure · In-nozzle flow visualization · Near-field spray dynamics

Abbreviations

SR	Synchrotron radiation
ESRF	European synchrotron radiation facility
APS	Advanced photon source
SPring-8	Super photon ring
IDs	Insertion devices
SSRF	Shanghai synchrotron radiation facility
GDI	Gasoline direct injection
SOI	Start of injection
SOC	Start of injection command
PIV	Particle image velocimetry
PDPA	Phase doppler particle analyzer

1 Introduction

Synchrotron radiation (SR) is a kind of electromagnetic radiation generated when the direction of movement of electrons traveling at almost light speed is altered by a magnetic field. This radiation is similar to other electromagnetic radiation, such as visible light and X-rays. However, the wave band of SR is primarily situated between infrared light and soft X-rays, and thus is on the same size scale as living cells, viruses and even atoms. Consequently, SR is a perfect light source for research involving exceptionally small objects. Compared to visible light, SR has many other advantages, including high brilliance, a broad spectrum, the capacity for a significant level of polarization and collimation, along with high photon flux, low emittance, the potential for pulsed emission, and energy and wavelength tuning. For all these reasons, SR has numerous applications in scientific research. For instance, Sun et al. [1] mapped strain distribution around nanostructures of oxides using scanning X-ray. Jiang et al. [2] discovered a crystalline phase of two-dimensional nanocrystal superlattices using in situ time-resolved X-ray.

The first-generation SR light sources were built with the aim of understanding the fundamental laws of matter

✉ Zhijun Wu
zjwu@tongji.edu.cn

[1] School of Automotive Studies, Tongji University, Shanghai 201804, China

and particle interactions. Several generations of scientists and engineers from all over the world participated in this endeavor [3]. As accelerator-based SR became more intense and its applications more promising, devices that enhanced the intensity of SR were built into existing rings. At present, there are an increasing number of SR sources throughout the world.

A SR light source consists of a linear accelerator (LINAC), a booster synchrotron, a storage ring, insertion devices and beamlines. The storage rings in third-generation SR light sources have been optimized in terms of the electron beam emission and insertion devices. Compared to the first- and second-generation devices, third-generation synchrotrons provide higher brilliance and are able to generate quasi-monochromatic light with partial coherence. According to the photon energy they provide, these units can be classified as high-, medium- or low-energy light sources. Third-generation synchrotron devices are ideal light sources for a wide range of fundamental research and studies related to technological innovation.

Over the last decade, the development of SR X-ray imaging technologies such as X-ray radiography, phase-contrast X-ray imaging, X-ray tomography and micro-computerized tomography (CT) has led to the application of SR to the study of fuel sprays [4, 5]. Wang et al. conducted a series of exploratory studies regarding fuel spray breakup using the APS at the Argonne National Laboratory [6–12]. This work initiated the application of SR X-ray techniques to research regarding spray breakup and atomization mechanisms. Wang et al. also successfully photographed the instantaneous microscopic morphologies of spray liquid cores at the nozzle outlets [13–16], and captured the propagation of spray-induced shock waves in a gaseous medium using SR together with a fast X-ray detector [17]. Moon [18] used this technology to observe significant differences in the dynamic structures of biodiesel and conventional fuel sprays, even under the same injection pressure. High-speed X-ray imaging has also been found to serve as a powerful tool for the assessment of velocity and density distributions inside a GDI spray in the near field [19]. The formation mechanism and control strategies of the fuel dribble from modern diesel injectors have also been investigated [20]. The results of such work demonstrate that increasing the injection pressure increases the population of the mode in which fast break up with a short fuel dribble residence time occurs.

X-ray imaging techniques have also been applied to the study of the structures [21, 22] and fuel flows inside nozzles [23, 24]. Moon et al. [25] investigated the structure and dynamics of the in-nozzle flow from a multi-hole GDI injector in conjunction with various nozzle hole geometries. The results indicated that the nozzle inlet structure had a significant effect on the flow in the orifice, and the imaging process provided very clear observations of the fluid cavitation and separation. Other researchers have performed numerical simulations using three dimensional (3D) models generated through high-energy X-ray micro-CT technique [26]. In another study, Wang et al. [27] determined nozzle and deposit morphologies using high-resolution X-ray microtomographic scans. In-nozzle flow simulations were subsequently performed, and the results indicated that the rough surfaces of the deposits led to additional cavitation and restricted the flow area, thus reducing the mass flow rate. Analyses of nozzle inner geometry parameters in this manner allows a comparison of nozzle orifice processing methods such as computerized numerical control drilling and electric discharge machining [28], with the aim of controlling the quality of diesel nozzle manufacture. In other work, in-nozzle needle motion characteristics were examined by Huang et al., utilizing X-ray phase-contrast imaging [29]. Komada and Moon [30] employed 80 ps X-ray pulses to visualize the transient needle motion and identified needle vibration during the injection process, with an amplitude that decreased over time.

SR X-ray imaging technology can also be utilized to precisely measure the internal structure of a nozzle, the needle movement, the internal flow and the breakup process of the near-field spray. The present review presents a systematic summary of the latest progress in engine fuel injection studies using SR X-ray imaging technology. This review is based on the recent work of the authors as well as other relevant work worldwide. This summary of recent research achievements is expected to assist in promoting the application of this advanced technique within the field of spray studies, so as to fully elucidate the spray breakup mechanism.

2 Third-Generation SR Light Sources

Third-generation SR light sources have been optimized to use insertion devices such as wigglers and undulators to obtain higher brilliance, low emittance beams, typically with brilliance values in excess of 10^{18} photons/s/mm^2/mrad^2/0.1%BW [31]. A large-scale SR facility is generally defined as one having an electron energy of more than 5 GeV and capable of delivering X-rays from undulators. At present, there are more than 50 SR sources in operation worldwide.

2.1 Main Third-Generation SR Light Sources Worldwide

The three highest energy large-scale storage ring synchrotron light sources are presently the ESRF in France, the APS in the USA and the SPring-8 in Japan. These facilities

Table 1 Representative parameters for the three largest high-energy SR light sources

	Energy (GeV)	Storage ring circumference (m)	Number of beamlines	Current (mA)	X-ray brilliance
ESRF	6	844	44	200	1×10^{21}
APS	7	1104	35	100	1×10^{20}
SPring-8	8	1436	57	100	1×10^{21}

Table 2 A comparison of some intermediate energy synchrotron light sources worldwide

	Location	Energy (GeV)	Storage ring circumference (m)	Number of beamlines	Current (mA)
SSRF	China	3.5	432	13	300
PLS	Korea	3	281	36	400
ANKA	Germany	2.5	110	20	110
ALS	US	1.9	197	12	400

generally produce light that is about one billion times more brilliant than that provided by conventional X-ray sources.

The ESRF began operation in 1994 as the first third-generation source providing extremely brilliant beams in the 100-nm to 1-μm size range. The APS and SPring-8 facilities, having similar performance and design parameters, came into service several years later (1996 and 1997, respectively). Table 1 compares the most representative parameters of these three largest light sources. The electron energy is a crucial factor that reflects the size and cost of the light sources and differentiates these three hard X-ray facilities from other much smaller light sources. All these three facilities have over 30 undulator beamlines open to public use and provide high-energy, high-brilliance and highly penetrating X-ray beams that are ideal for studying the arrangements of molecules and atoms, probing the interfaces where materials meet, determining the interdependent form and function of biological proteins, and tracking chemical processes that occur on the nanoscale.

These higher energy facilities are complemented by other lower cost, intermediate energy light sources that have gradually been built around the world. Some representative light sources are described in Table 2, among which the Shanghai Synchrotron Radiation Facility (SSRF) is one of the best. The SSRF provides SR X-ray in a wave band between the infrared and hard X-ray regions of the spectrum. This facility commenced operation in 2009 with an electron energy of 3.5 GeV and a capacity of 13 beamlines, and is currently the highest performance third-generation intermediate energy SR source.

2.2 Imaging Beamlines for Fuel Injection Studies at the SSRF

Presently, within the field of fuel spray research, there is a significant focus on the spray breakup mechanism and its interplay with the nozzle internal flow characteristics. To understand the nozzle internal flow characteristics, static measurements of the internal structural parameters of the nozzle and dynamic assessments of the effect of the 3D needle motion are both necessary, while the transient spray morphology measurement is spray breakup mechanism. Various X-ray imaging techniques and corresponding experimental beamline setups, respectively, must be developed for these purposes.

Table 3 Specific technical parameters of the BL13W1 beamline

Photon energy range	8–72.5 keV
Beam size	45 mm (H)×5 mm (V) @ 34 m @ 20 keV
Flux output	5×10^{10} phs/s/mm^2 @ 20 keV @ Si (111)
	2×10^{8} phs/s/mm^2 @ 70 keV @ Si (311)
Pixel size range	0.32–24 μm
Energy resolution	$<5\times10^{-3}$

The X-ray Imaging and Biomedical Applications Beamline (BL13W1) at the SSRF is one of the first beamlines applied to fuel injection research, and the technical parameters of this beamline are presented in Table 3. Both micro-CT and in-line phase-contrast imaging can be performed at this facility, as means of examining the inner microstructures of fuel injectors.

An X-ray white beam test beamline is currently under construction at the SSRF and will be available for the testing and verification of ultrafast imaging equipment and methods. As part of a joint endeavor, our research group has already performed analyses of GDI injector needle motion at this beamline, employing a customized aluminum GDI injector, as shown in Fig. 1. The results have demonstrated the lifting process of the needle valve as well as its eccentric vibration.

Analyses of the GDI spray near-field characteristics have also been conducted at this beamline. Using a

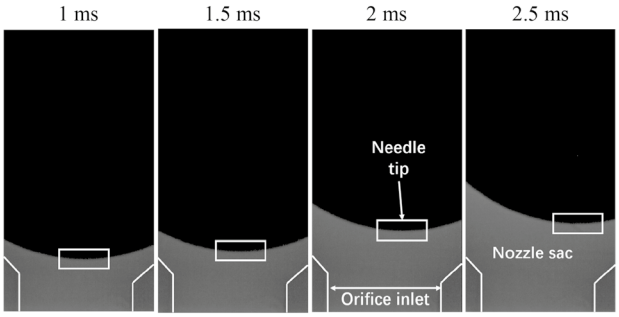

Fig. 1 Images of a GDI injector needle motion process acquired at the SSRF

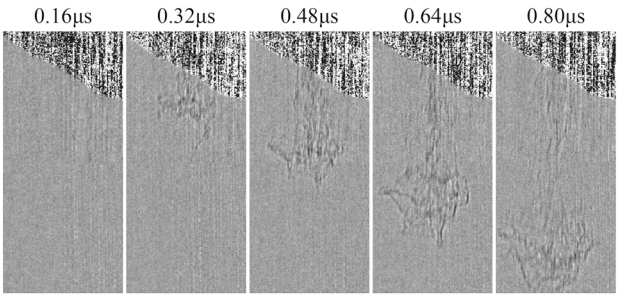

Fig. 2 Images showing the near-field spray liquid core development process, acquired at the SSRF

Table 4 Design parameters for the SSRF ultrafast X-ray imaging beamline

Photon energy range	8.7–30 keV
Energy resolution	2×10^{-4} @10 keV
Beam size	1.5×1.0 mm^2 @ 10 keV
Flux output	1×10^{13} phs/s @ 10 keV@300 mA
	5×10^{15} phs/s @ 300 mA (white beam)
	1×109 phs @ 20 mA (single pulse)
Time resolution	80 ps
Spatial resolution	1 μm

160-ns exposure time, the development of the spray liquid core under a 1-MPa injection pressure was tracked, as depicted in Fig. 2. To maintain the imaging intensity with this beamline, it was necessary to use a minimum exposure time and so the precision of the spray trajectory image is not optimized due to the limited flux output of the beamline.

The SSRF Phase II beamline project, involving the addition of 16 new beamlines, was approved in 2015, and an ultrafast X-ray imaging beamline with a higher flux output and improved time resolution is now under construction. The associated design parameters (as shown in Table 4) are in line with the highest international standards and are comparable to those of the ESRF, APS and SPring-8 facilities in terms of energy range as well as temporal and spatial resolution.

3 Effects of Nozzle Internal Structure on Fuel Injection Characteristics

To date, a number of research results have demonstrated that the nozzle internal flow conditions, which in turn depend on both the static and dynamic boundary conditions, play a critical role in the spray development characteristics. The static boundary conditions of the nozzle internal flow, which are associated with the nozzle internal structure, can be assessed nondestructively by micro-CT imaging technique.

3.1 Nozzle Three Dimensional Internal Structure Analyses by X-ray Micro-CT

The internal geometric parameters of a nozzle, including the length and diameter of nozzle orifices, the *k* factor, the orifice inlet chamfer radius and the orifice surface characteristics [21], are key factors affecting the internal flow. As shown in Fig. 3, with the micro-CT scanning method and the corresponding data processing procedure, the actual digital model of the nozzle geometry could be generated via 3D reconstruction technique. During the scan process, the nozzle is held on a specimen rotating platform and the X-rays penetrate its tip before impacting a scintillator. A total of 720 images are recorded using a charge coupled device (CCD) camera at 0.25° rotation intervals. These absorption images are then converted into slices through a reconstruction process to produce a 3D digital model of the nozzle (Fig. 3b).

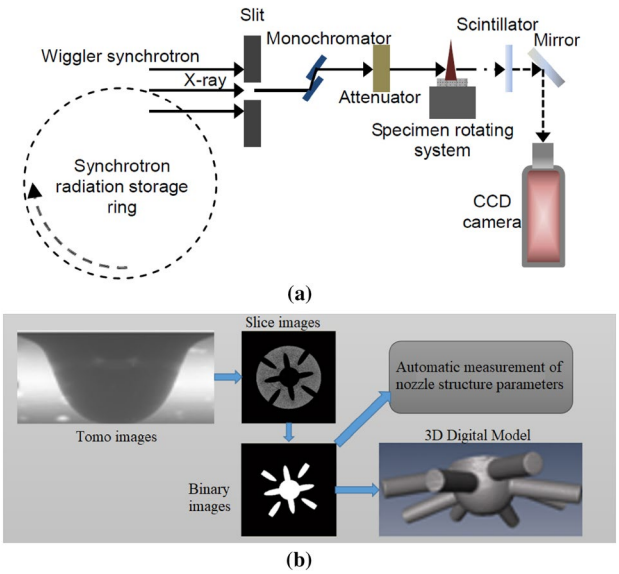

Fig. 3 The nozzle tip inner structure CT scan and data processing procedure [32]

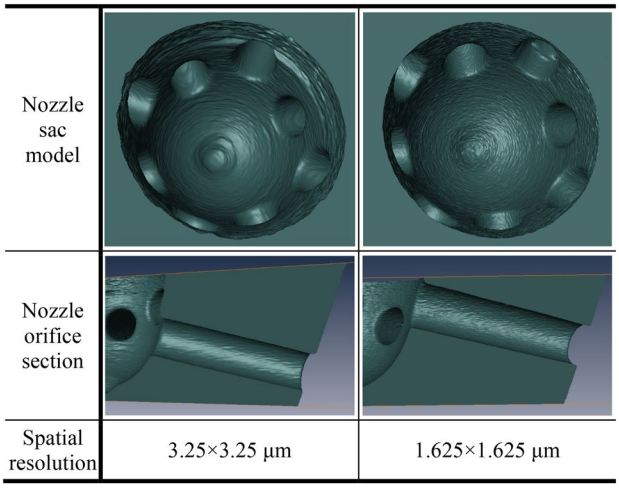

Fig. 4 Comparison of 3D digital models obtained with different spatial resolutions

Automatic measurement of the nozzle structure parameters [32] can be performed with specialized image processing programs based on binary slice images. Furthermore, the reconstructed model can be imported into computational fluid dynamics software to provide the geometric boundary inputs to generate a 3D computational mesh that can reflect the effect of the nozzle surface roughness and unevenness.

The actual spatial resolution of the resulting 3D digital model can be adjusted by varying the coupling between the CCD camera and the objective lens. Figure 4 presents a comparison of 3D digital models acquired with different spatial resolutions. It is evident that more information regarding the nozzle surface characteristics is captured with a higher spatial resolution (1.625 × 1.625 μm), although this requires a longer data acquisition time (> 10 h).

3.2 Numerical Research of Fuel Injection Characteristics based on Actual Nozzle 3D Geometries

Before X-ray micro-CT technique was applied to the assessment of nozzle internal structures, fuel flow simulations were generally based on simplified and idealized geometric models according to the nozzle design parameters, which can be quite different from the actual nozzle structure. Therefore, such simulations would have inevitable deviations from the actual flow characteristics, due to a lack of information regarding the true 3D nozzle geometry.

Wu et al. [33] compared the nozzle orifice wall pressure distributions in the azimuthal direction obtained from two-dimensional (2D) and 3D simulations, as shown in Fig. 5. Two single-hole nozzles are tested, respectively, and one has not been hydraulically grounded, defined as Nozzle-NEG (non-hydro erosive grinding), while the other

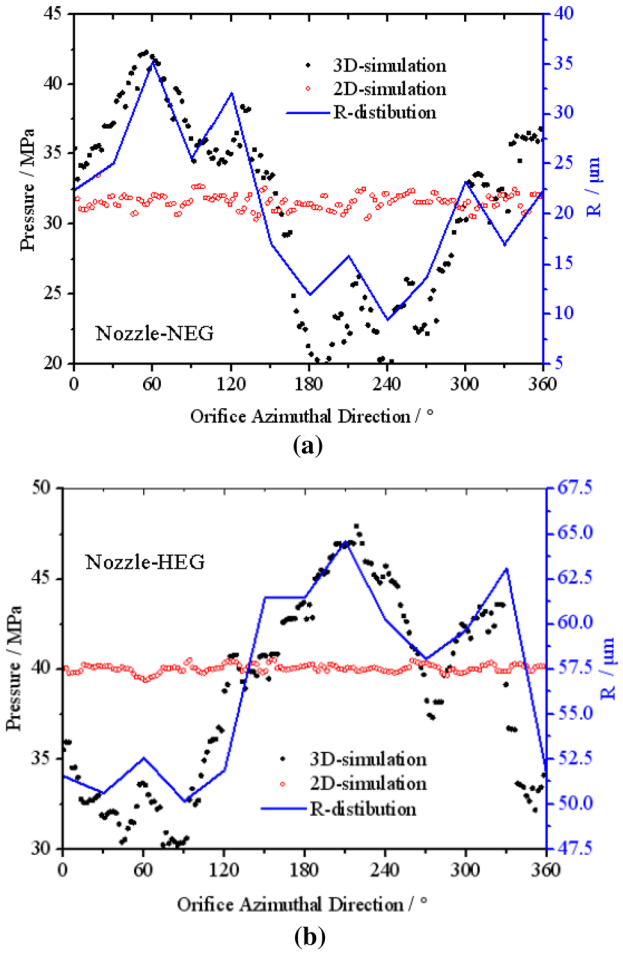

Fig. 5 Comparison of pressure distributions between 3D and 2D simulations [33]

has been hydraulically grounded and therefore has larger inlet rounding radius value, defined as Nozzle-HEG (hydro erosive grinding). The results indicated that the pressure remained almost constant in the 2D simulation, while the 3D results exhibited gradual changes in accordance with the inlet rounding radius of the 3D model for both of the two nozzles. This phenomenon demonstrated that the rounding radius of the orifice inlet has a significant effect on the pressure distribution at the orifice and also confirmed that 2D simulations can introduce large errors when calculating the nozzle internal flow.

A simulation of cavitation in the nozzle (as shown in Fig. 6) further verified that the orifice rounding radius has a significant effect on the nozzle internal flow. In the case of the actual 3D model, the inner flow characteristics were quite different from those in the ideal model, especially the cavitation formation near the inlet area [34].

Given the high degree of correlation between the orifice inlet rounding radius and the internal flow conditions, the impact of this geometric factor on the spray characteristics

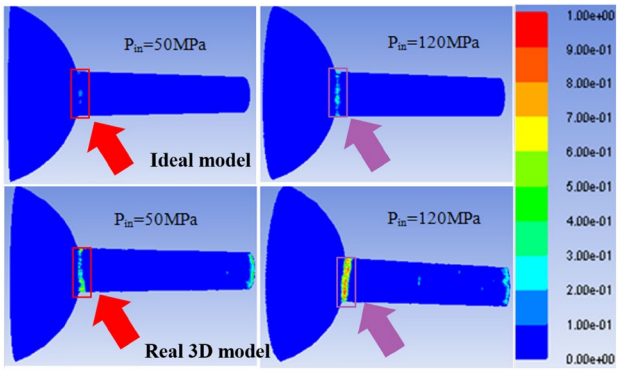

Fig. 6 Simulation results for cavitation distribution based on actual and ideal 3D models [34]

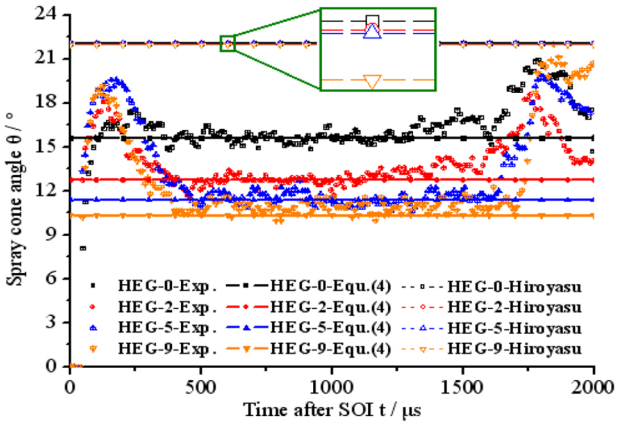

Fig. 7 A comparison of experimental and predicted spray cone angles at $P_{in}=90$ MPa, $P_b=3$ MPa [35]

was further investigated [35]. The results indicated that, during the steady state of the spray, the difference in spray behavior exhibited by nozzles with different hydro erosive grinding (HEG) times was significant, as demonstrated in Fig. 7. The standard deviation of the orifice inlet rounding radius, σ, was introduced to revise the classical empirical correlation between the spray cone angle, θ, and the nozzle orifice structural parameters (orifice length, L, inlet and outlet diameters, D_{in} and D_o, and the ambient air to fuel density ratio, ρ_a/ρ_l). A new correlation was proposed that takes into account the effect of the orifice inlet rounding radius on the steady state, written as:

$$\theta = k_1 \cdot \sigma + k_2 \left(\frac{L}{D_{in}}\right)^{-0.22} \cdot \left(\frac{D_{in}}{D_o}\right)^{0.15} \cdot \left(\frac{\rho_a}{\rho_l}\right)^{0.26} + b \quad (1)$$

From Fig. 7, it is apparent that the new correlation can better predict the steady-state spray cone angle, and such predictions have shown excellent agreement with the experimental data obtained under a 90-MPa injection pressure P_{in} and 3-MPa ambient pressure P_b.

4 The Effect of Dynamic Needle Motion on Fuel Injection Characteristics

A significant body of research has demonstrated that the needle valve is not only a switch to control the opening and shut off of the fuel flow inside the injector, but also has a significant effect on the spray morphology and other characteristics. Both the needle lift motion and its eccentric vibration, which are defined as the dynamic boundary conditions for the nozzle internal flow, directly impact the nozzle internal flow characteristics during the injection process. Therefore, it is necessary to obtain precise visualizations of the 3D motion of the needle valve during the injection process. Ultrafast X-ray phase-contrast imaging allows precise observations of the cavitation formation process inside the nozzle sac volume as well as the needle 3D motion.

4.1 Needle Motion Measurement by Ultrafast X-ray Phase-Contrast Imaging

The main injector internal moving parts include the needle valve, check valve and armature (Fig. 8). The motion of these parts directly affects the injection delay and the injection flow rate characteristics. However, these components are quite difficult to examine nondestructively since they are covered by the thick metal shell of the injector.

As an example, the thickness of the nozzle lower end is generally greater than 3 mm, while that of the upper end is more than 5 mm, which makes the imaging and analysis of needle motion quite challenging. Before SR X-ray imaging technique was applied to the measurement of needle motion, a precise 3D needle motion profile was very difficult to obtain. The conventional measurement methods, such as those using inductive displacement transducers, fiber-optic

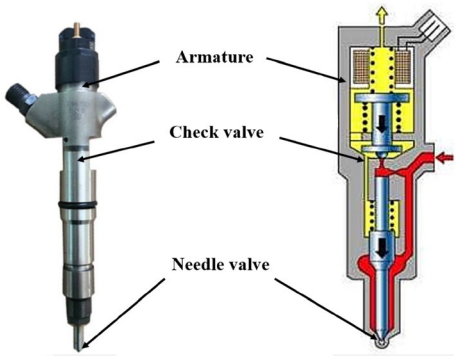

Fig. 8 The internal moving parts of a diesel nozzle

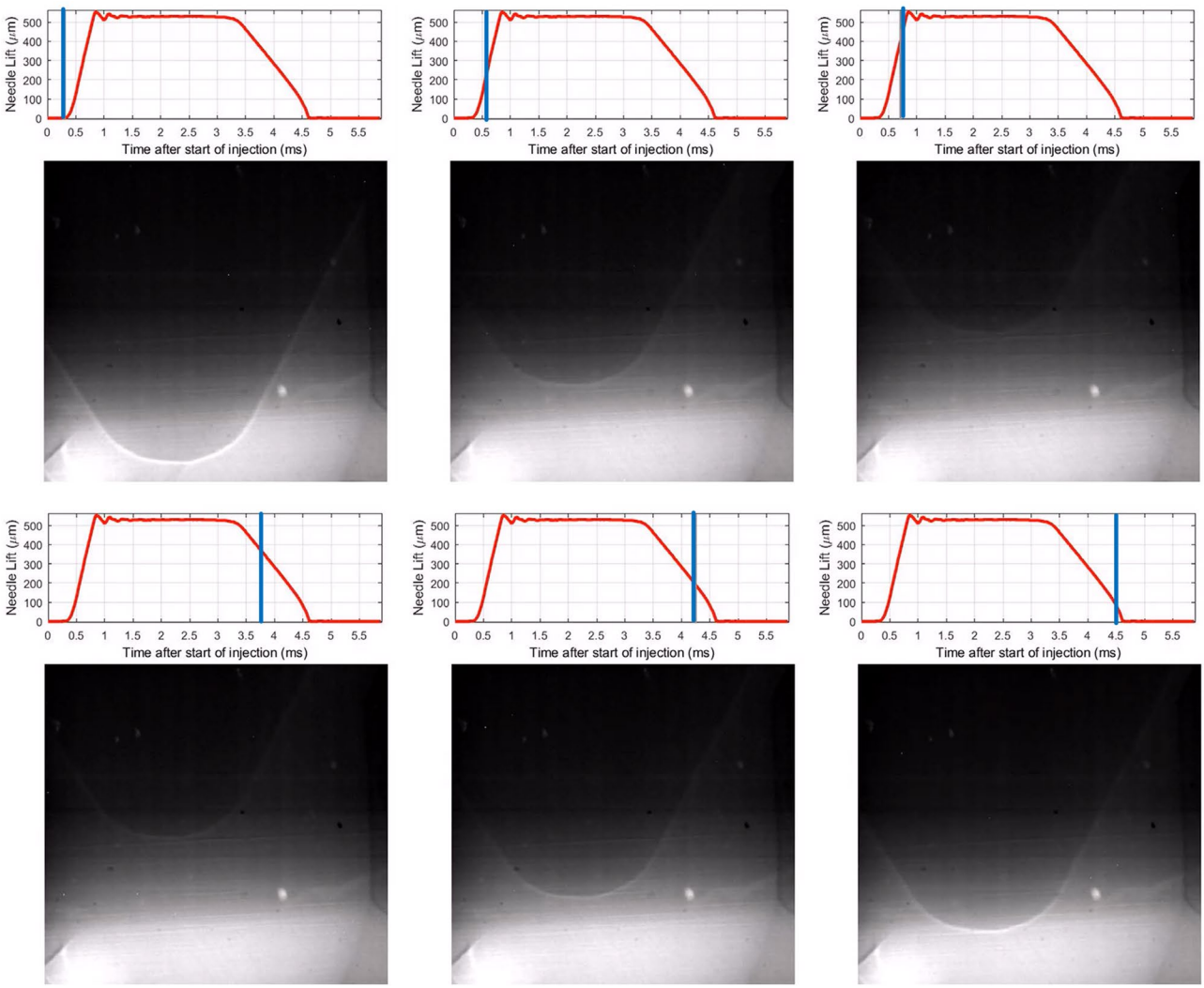

Fig. 9 Visualization of the entire needle motion process of a diesel injector

displacement sensors or laser displacement sensors, all have inevitable limitations. In contrast, X-ray imaging has the advantages of producing no electromagnetic interference, is nondestructive, allows high precision analyses and can be used to monitor moving parts without any changes to the original injector structure.

High-energy, high-flux SR X-ray imaging is also the only nondestructive method that can track the dynamic motion of these parts. Using ultrafast X-ray phase-contrast imaging technique, the diesel injector needle motion during the entire injection duration has been recorded, as shown in Fig. 9.

4.2 Research Regarding the Effects of Needle Movement on Spray Characteristics

Many numerical studies of fuel injection characteristics have been performed, based on static simulations with fixed needle lift heights. These simulations result in non-negligible variations from the actual situation. A number of investigations have reported that the maximum lift height of the needle valve in the steady state is not the only factor that affects the spray characteristics. In fact, the dynamic characteristics of the needle lift process also have a significant impact on spray development.

Because the fuel flow between the needle tip and the valve seat is directly related to the needle lift height, it determines the flow speed and pressure gradient between the upstream high-pressure fuel channel and the nozzle sac. Thus, the local pressure increment inside the nozzle sac volume is correlated with the dynamic needle lift process. The local pressure of the sac volume gradually increases as the needle valve moves upward, eventually reaching the nominal injection pressure as the needle moves to its maximum lift height. The fuel velocity at the nozzle exit, which is determined by the pressure difference between the inlet and outlet of the nozzle orifice, would thus undergo a similar

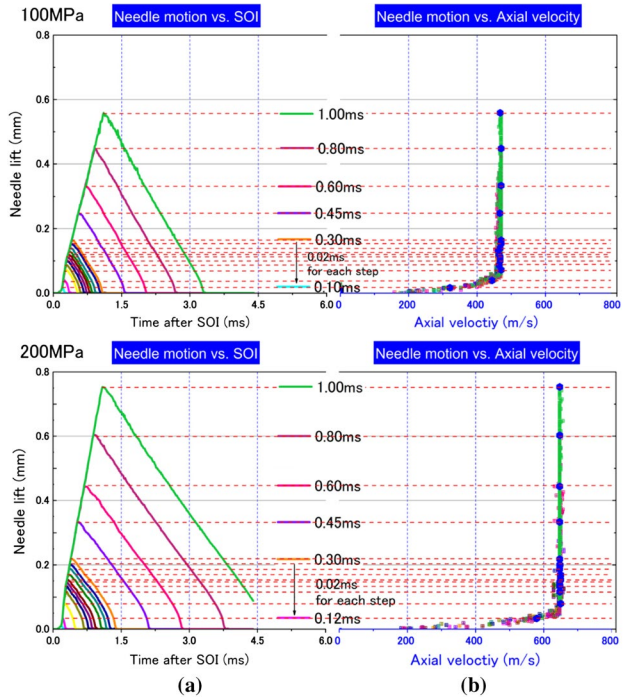

Fig. 10 Changes in the liquid jet dynamics with needle lift for different injection pulse durations: **a** needle lift versus time after SOI and **b** needle motion versus axial velocity [29]

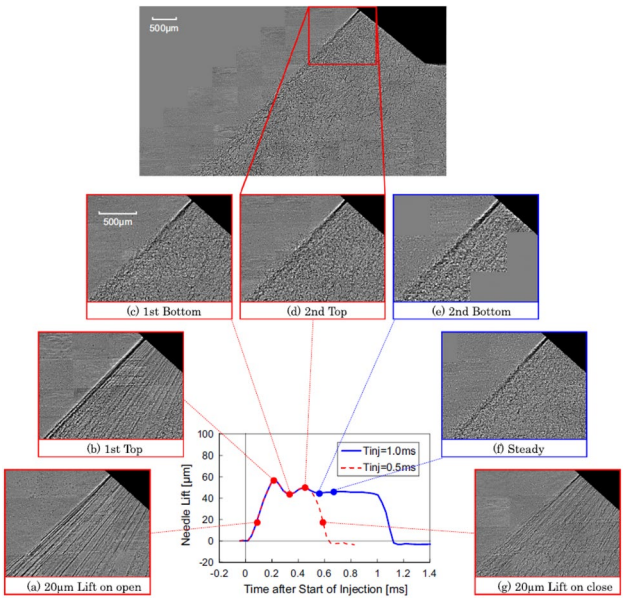

Fig. 11 Near-field spray morphology images acquired at different stages of fuel injection [30]

increase. Research regarding the relationship between needle lift dynamics and spray jet velocity by Huang et al. [29] has demonstrated this effect in detail. According to the results displayed by Fig. 10, the axial velocity increases exponentially during the initial needle-opening stage in conjunction with various injection pulse durations and becomes constant after the needle reaches a certain critical height. Once this steady state is achieved, the jet axial velocity remains unchanged even with further increases in the needle lift.

Komada et al. [30] investigated the effect of the transient needle motion on the initial spray formation, using X-ray phase-contrast imaging technique. An obvious needle vibration was found to result in perturbation of the near-nozzle flow and thus to alter the spray intact liquid length and flow breakup. Figure 11 shows near-field spray morphology images acquired at various fuel injection stages. These results demonstrate that the near-field spray was barely perturbed during the initial needle-opening stage, while the flow perturbation and spray breakup were substantially enhanced at the maximum needle lift because of the higher injection velocity and nozzle internal turbulence intensity.

The eccentric vibration of the needle is also an important contributor to internal flow perturbation and hole-to-hole spray unevenness in modern fuel injectors. Utilizing X-ray phase-contrast imaging technique, Moon et al. [36] analyzed the relationship between eccentric needle motion and the near-nozzle spray dynamics of diesel nozzles with different

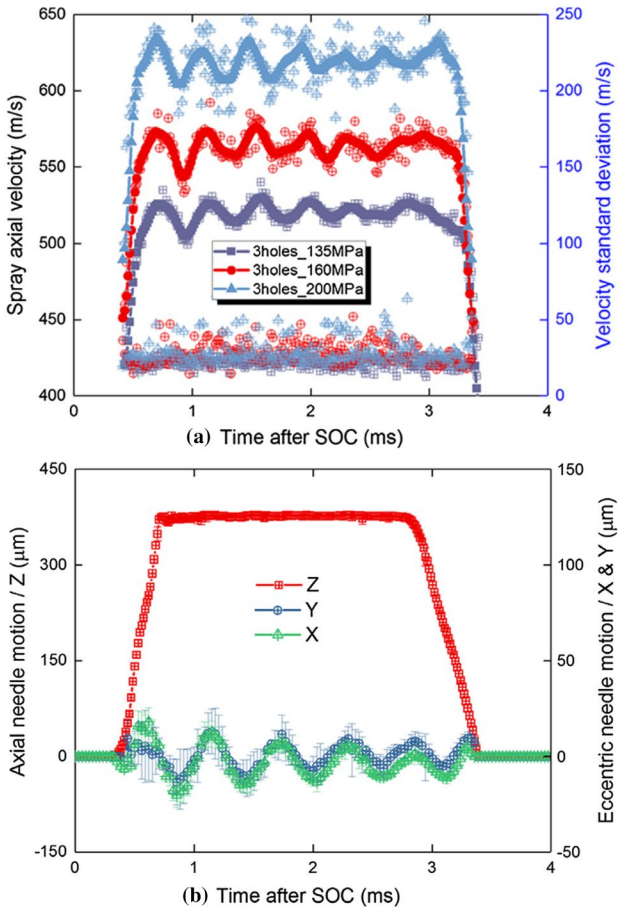

Fig. 12 **a** Spray axial velocity values and **b** axial needle motion as functions of time after SOC [36]

hole numbers. The eccentric needle motion and near-nozzle spray axial velocity exhibited temporal oscillations during the injection, as illustrated by Fig. 12. Both oscillations showed similar trends using various nozzles and injection pressures, indicating the mutual dependency of these two oscillations.

5 Visualization of the Nozzle Internal Flow and Fuel Spray Characteristics

Based on numerous studies using conventional optical measurement techniques such as high-speed photography, Schlieren imaging, PIV and PDPA, the automotive industry has already gained a relatively comprehensive understanding of spray secondary atomization, fuel droplet vaporization and in-cylinder mixture formation [37–39]. However, due to the limited penetration of visible light into high-density liquid fuel, conventional optical measurement methods can only capture the overall profile of the spray liquid core. Thus, optical techniques cannot examine the transient microscopic characteristics of the spray primary breakup process. Because spray breakup is affected to a great extent by in-nozzle cavitation and turbulence, the flow inside the nozzle orifice has mainly been monitored using transparent nozzles. Even so, due to the differences between such test nozzles and the actual devices (such as pressure endurance and surface characteristics), the reliability of research results based on transparent nozzles is still uncertain.

Therefore, visualization of the nozzle internal flow characteristics and precise quantification of the spray liquid core region are the main difficulties associated with studying the high-pressure injection fuel atomization mechanism.

5.1 Visualization of Nozzle Internal Flow Characteristics

As the nozzle sac volume is enclosed by thick metal housing and the entire injection process occurs within microseconds, traditional optical techniques cannot be used to examine in-nozzle flow characteristics or fuel cavitation. In contrast, SR X-ray phase-contrast imaging can clearly capture the liquid–gas interface and thus reveal the process by which cavitation bubbles appear. Therefore, this technique could be used to assess the 3D two-phase flow characteristics inside the injector nozzle.

The effect of the nozzle internal structure on the spray characteristics, as discussed in Sect. 3, is believed to be primarily due to fuel cavitation and flow unevenness inside the nozzle sac and orifices. The SC X-ray phase-contrast imaging results have confirmed this hypothesis. Figure 13 presents images of the fuel flow characteristics in the in-nozzle and near-field spray regions of a GDI injector, showing

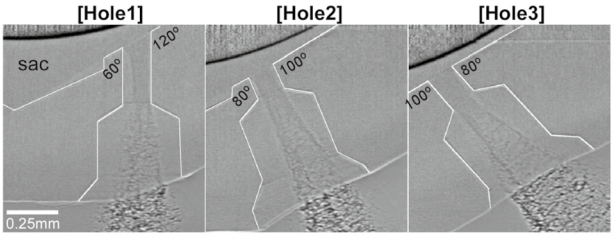

Fig. 13 Visualization of the fuel flow within the in-nozzle and near-field spray regions [25]

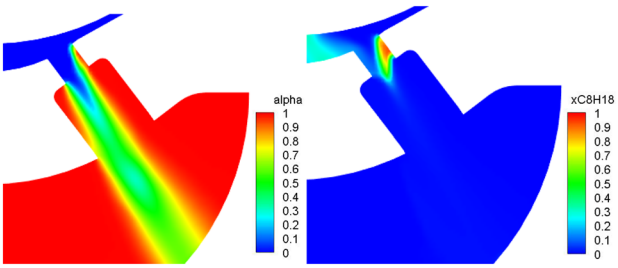

Fig. 14 Numerical simulations of the void fraction (alpha) and fuel vapor mole fraction (xC8H18) distribution along an axial section of a nozzle orifice

obvious boundary layer separation phenomenon at the upper end of the nozzle orifice.

Such boundary layer separation is typically ascribed to significant cavitation at the geometric contraction region of the flow path. Recent simulations by our own group (Fig. 14) indicate a similar flow separation phenomenon based on the void fraction distribution contour along an axial section of the nozzle orifice. The distribution contour of fuel vapor mole fraction (indicated by xC8H18 in Fig. 14) also confirms a high degree of cavitation resulting from fuel vaporization, which causes flow separation at the upper end of the nozzle orifice.

Moon et al. [25] investigated the in-nozzle flow characteristics of GDI gasoline nozzles with various hole structures, as shown in Fig. 15. The results showed that the structure of the nozzle inlet had a pronounced effect on the internal flow characteristics, and fluid cavitation and separation caused by the structure could be clearly observed.

By conducting a comprehensive analysis of the relationship between the in-nozzle flow characteristics (such as cavitation area and location, flow separation and turbulence) and the spray jet velocity distribution, the interaction between the internal flow and the spray characteristics with different nozzle structures can be elucidated.

The injection pressures in diesel injectors can be greater than 200 MPa, and thus much higher than those in a GDI injector. Consequently, the cavitation mechanism during the injection process could be very different. Indeed, studies

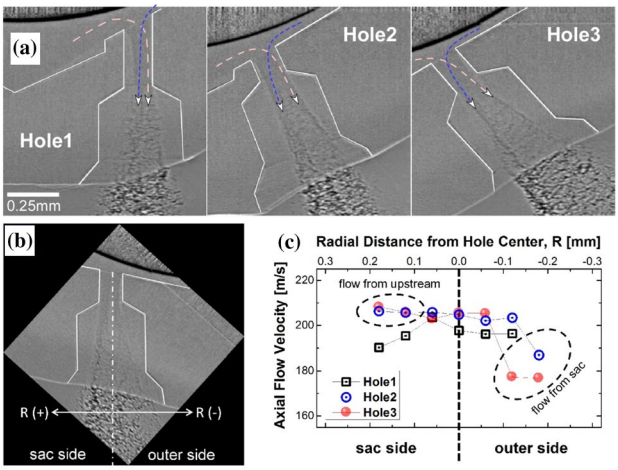

Fig. 15 SR X-ray imaging of the in-nozzle flow and emerging jet flow of a GDI nozzle: **a** in-nozzle and emerging jet flow, **b** the location at which the emerging jet flow dynamics were examined (along line *R*) and **c** the emerging jet flow dynamics at each hole [25]

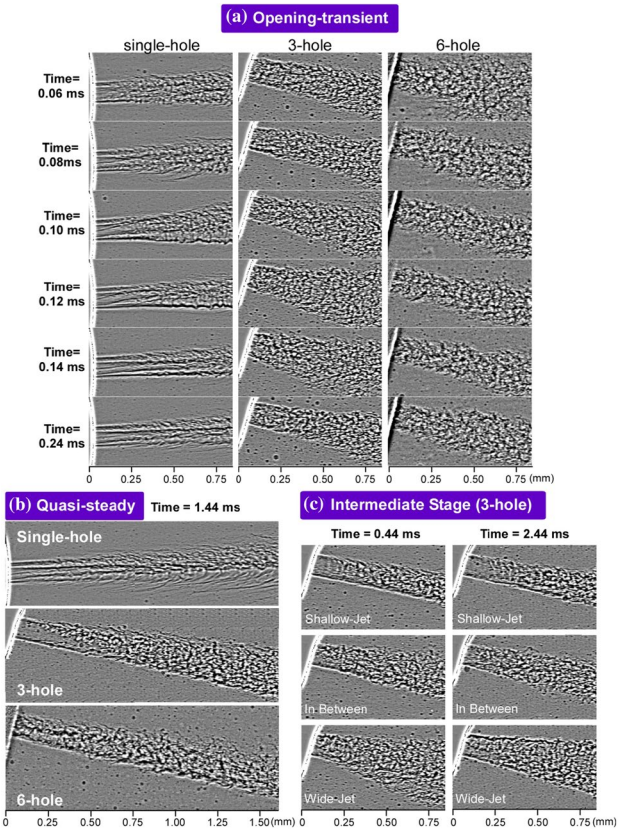

Fig. 16 Fuel spray morphology images obtained with ultrafast X-ray phase-contrast imaging [40]

have shown that the entire injector sac wall and the orifice inlet may be damaged by the bursting of cavitation bubbles. Therefore, the visualization of such processes is crucial to understanding the cavitation formation mechanism and to devising means of suppressing cavitation bubbles to improve the injector durability.

5.2 Visualization of Fuel Spray Morphology and Dynamic Characteristics

The imaging of the spray near-field liquid core morphology is very important to understand the spray development process as well as the breakup and atomization mechanism of the liquid core. As shown in Fig. 16, ultrafast X-ray absorption and phase-contrast imaging can monitor the near-field spray liquid core morphology with high spatial and temporal resolution [40]. However, it is still challenging to obtain quantitative information from such spray morphology images to study the fuel spray characteristics.

The distribution of the spray velocity field in the near-nozzle region reflects changes in the spray momentum and kinetic energy, and can provide information regarding the breakup mechanism of the spray liquid core. Such knowledge is necessary for further optimization of fuel injectors to meet increasingly stringent emissions regulations. Near-field spray velocity data can be obtained using a multiple exposure X-ray technique. In this method, the spray region of interest (ROI) is exposed to three X-ray pulses with 11 mA current, 17 ns width and 68 ns period (see Fig. 17a) and the resulting triple-exposed images are divided into small interrogation windows (see Fig. 17b) to allow velocity calculations. An autocorrelation analysis is then performed in a particular ROI as depicted in Fig. 17c [18]. The peak correlation points are located in the interrogation window, and the velocity vector can be obtained as the ratio of the spatial interval between peak points (22.5 μm) to the exposure time interval (68 ns).

The fuel spray density distribution in the liquid core region is another critical factor that can provide information regarding the spray breakup dynamics, since it reflects the extent of air entrainment by the liquid jet. Spray densities can be determined using quasi-monochromatic X-rays extracted from the original white beam according to the Bragg–Gray principle.

Figure 18a shows the two processes used for density evaluations. The raw image is first corrected by subtracting a blank background acquired without a spray. A median filter is then applied to the background corrected image. The measurement setup is calibrated using cannulas of different diameters filled with n-heptane. Based on the density of n-heptane and the size of the cannulas, the

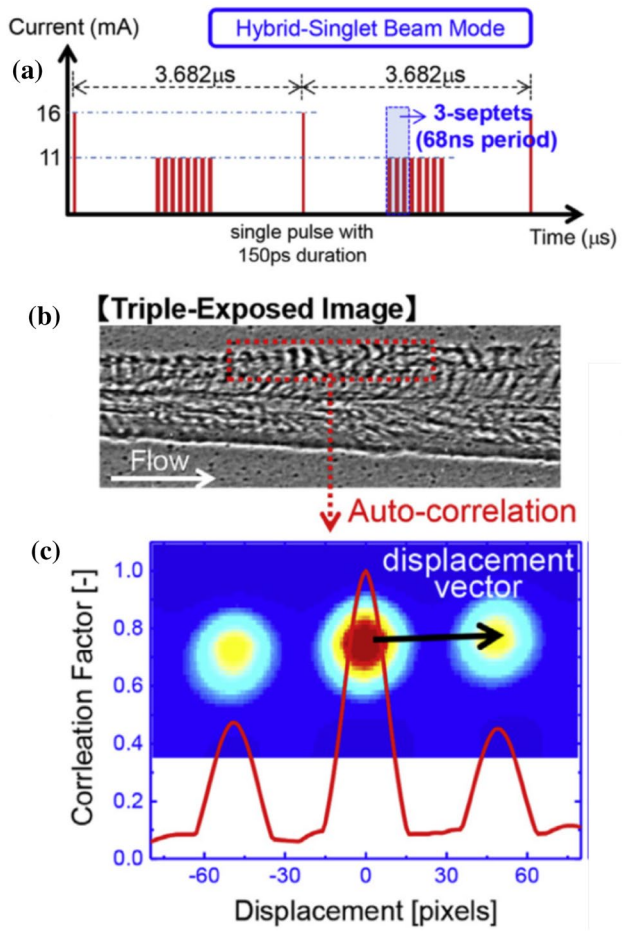

Fig. 17 **a** X-ray beam pattern used for triple-exposed imaging, **b** sample of triple-exposed X-ray phase-contrast image and **c** color-map and profile of correlation factor derived from the autocorrelation analysis of triple-exposed image [18]

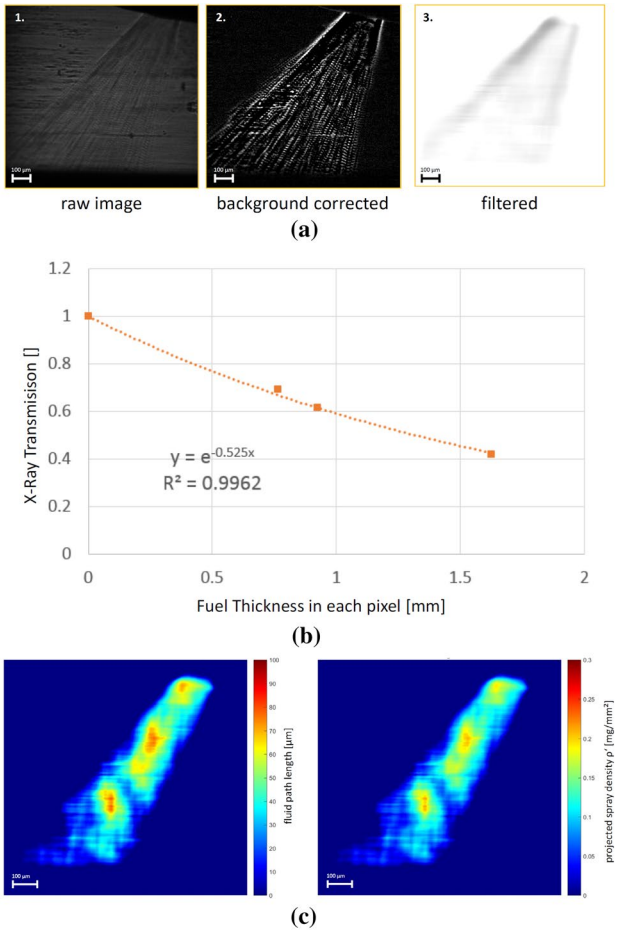

Fig. 18 **a** The basic process of spray density evaluation algorithm, **b** calibration result of the X-ray transmission as a function of fuel thickness and **c** example for the spray density evaluation, left: fluid path length the X-ray is passing; right: projected spray density [19]

transmission coefficient can be calculated by applying the Lambert–Beer–Bonquer law. Figure 18b plots the X-ray transmission as a function of the thickness of the n-heptane samples. The density distribution inside the spray is subsequently calculated by applying the calibration coefficient to the image, as shown in Fig. 18c [19].

The hole number and location of the nozzle orifices both have a significant effect on the spray morphology, and the nozzle structure is one of the most important factors affecting the spray liquid core breakup process. Zhang et al. [13] investigated the near-field spray morphologies of diesel injectors with different nozzle orifice placements, using fast X-ray phase-contrast imaging. As shown in Fig. 19, the experimental results indicated that the maximum spray width of a two-hole injector was over twice that of a single-hole injector, and a vortex flow was induced by increasing the nozzle orifice umbrella angle (UA).

The interaction between the ambient air and the nozzle exit spray jet is the dominant factor determining the subsequent breakup process and the downstream vortex structure of the fuel spray. However, the effects of the ambient air density on the spray characteristics have not been thoroughly examined in previous studies.

Jeon et al. [41] have related the spray breakup length to the ambient air density to determine a detailed spray atomization mechanism. The results indicate that an increase in the ambient density decreases the breakup length of the liquid sheet. However, this effect becomes insignificant as the initial flow turbulence is increased in conjunction with high needle lift conditions, as shown in Fig. 20.

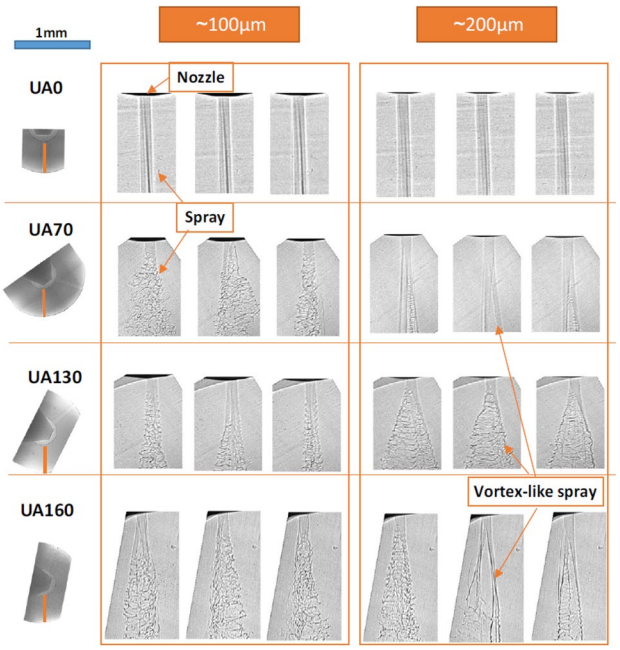

Fig. 19 Comparison of the spray morphologies of diesel injectors with different nozzle structures [13]

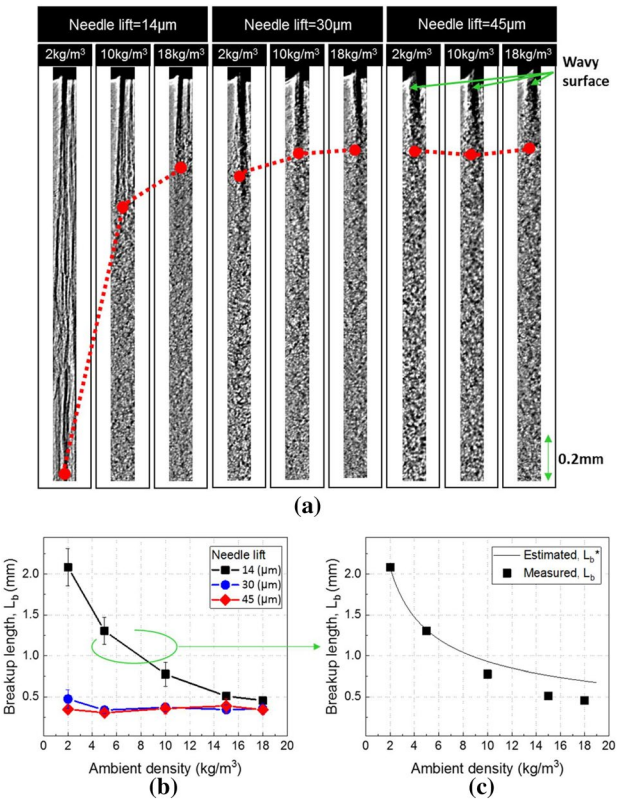

Fig. 20 Ambient density and needle lift effects on liquid-sheet breakup length: **a** images of the near-nozzle spray edge, **b** the breakup length data and **c** a comparison of breakup length results from the current measurements and predictions from a previous model. Data acquired under steady-state conditions (0.8 ms after SOI) [41]

6 Conclusions

This paper reviewed the application of SR X-ray imaging to the study of fuel injection characteristics. Representative parameters associated with primary third-generation SR light sources worldwide were compared. In addition, recent progress in the research of fuel injection characteristics by our group at the SSRF and the APS was briefly summarized. The operating principles of different X-ray imaging techniques as applied to the study of fuel injection and the latest relevant research progress were also described. The highlights of this research are as follows.

1. Micro-CT scanning and 3D reconstruction technology can be used to obtain true digital models of a nozzle that show the effects of the nozzle internal geometry on the in-nozzle flow characteristics under real-world conditions.
2. Using ultrafast X-ray phase-contrast imaging, internal cavitation and needle 3D motion can be visualized. The research results indicate that both the needle lift motion and eccentric vibration affect the nozzle internal flow characteristics.
3. The near-field spray morphology can be monitored using ultrafast X-ray phase-contrast imaging technique with high spatial and temporal resolution. Using X-ray multiple exposure and quasi-monochromatic X-ray absorption techniques allows the near-field spray velocity and density distribution to be obtained for quantitative analysis of the spray dynamics.

SSRF Phase II beamlines with higher flux outputs and improved time resolution are now under construction. The design indexes of these units are in keeping with the highest international standards in terms of energy range. Based on the upcoming ultrafast X-ray imaging beamline, further investigation of spray morphology and spray dynamics could be conducted at the SSRF. With ongoing improvements of X-ray beamlines, additional advances in the study of the spray breakup mechanism are expected. Based on collaboration with the industrial community, these advances should promote the application of more advanced injection techniques that will reduce both engine fuel consumption and emissions.

Acknowledgements This study was supported by the National Natural Science Foundation (U1832179) and as a Key Project of the SSRF (2016-SSRF-ZD-004512). The authors are sincerely grateful for the technical assistance and the contributions to this research from the staff of the BL13W1 beamline at the SSRF and SECTOR 7ID-B at the APS. The assistance of the Wuxi Fuel Injection Equipment Research Institute during injector manufacturing and modification is also gratefully acknowledged.

Compliance with Ethical Standards

Conflict of interest On behalf of all authors, the corresponding authors state that there is no conflict of interest.

References

1. Sun, T., Pan, Z., Xie, S., et al.: High-sensitivity strain mapping around epitaxial oxide nanostructures using scanning X-ray nanodiffraction. Appl. Phys. Lett. **98**(25), 251914 (2011)
2. Jiang, Z., Lin, X.M., Sprung, M., et al.: Capturing the crystalline phase of two-dimensional nanocrystal superlattices in action. Nano Lett. **10**(3), 799–803 (2010)
3. Bilderback, D.H., Elleaume, P., Weckert, E.: Review of third and next generation synchrotron light sources. J. Phys. B At. Mol. Opt. Phys. **38**(9), S773 (2005)
4. Knorsch, T., Mamaikin, D., Leick, P., et al.: Comparison of shadowgraph imaging, laser-Doppler anemometry and X-ray imaging for the analysis of near nozzle velocities of GDI fuel injectors. SAE Technical Paper 2017-01-2302
5. Kastengren, A., Powell, C.F., Arms, D., et al.: The 7BM beamline at the APS: a facility for time-resolved fluid dynamics measurements. J. Synchrotron Radiat. **19**(4), 654–657 (2012)
6. Im, K.S., Cheong, S.K., Powell, C.F., et al.: Unraveling the geometry dependence of in-nozzle cavitation in high-pressure injectors. Sci. Rep. **3**, 2067 (2013)
7. Wang, Y., Liu, X., Im, K.S., et al.: Ultrafast X-ray study of dense-liquid-jet flow dynamics using structure-tracking velocimetry. Nat. Phys. **4**(4), 305 (2008)
8. Im, K.S., Cheong, S.K., Liu, X., et al.: Interaction between supersonic disintegrating liquid jets and their shock waves. Phys. Rev. Lett. **102**(7), 074501 (2009)
9. Liu, X., Im, K.S., Wang, Y., et al.: Four dimensional visualization of highly transient fuel sprays by microsecond quantitative X-ray tomography. Appl. Phys. Lett. **94**(8), 084101 (2009)
10. Im, K.S., Fezzaa, K., Wang, Y.J., et al.: Particle tracking velocimetry using fast X-ray phase-contrast imaging. Appl. Phys. Lett. **90**(9), 091919 (2007)
11. Wang, Y.J., Im, K.S., Fezzaa, K., et al.: Quantitative x-ray phase-contrast imaging of air-assisted water sprays with high Weber numbers. Appl. Phys. Lett. **89**(15), 151913 (2006)
12. Cai, W., Powell, C.F., Yue, Y., et al.: Quantitative analysis of highly transient fuel sprays by time-resolved X-radiography. Appl. Phys. Lett. **83**(8), 1671–1673 (2003)
13. Zhang, X., Moon, S., Gao, J., et al.: Experimental study on the effect of nozzle hole-to-hole angle on the near-field spray of diesel injector using fast X-ray phase-contrast imaging. Fuel **185**, 142–150 (2016)
14. Lin, K.C., Rajnicek, C., Mccall, J., et al.: Investigation of pure- and aerated-liquid jets using ultra-fast X-ray phase contrast imaging. Nucl. Inst. Methods Phys. Res. A **649**(1), 194–196 (2011)
15. Liu, Z., Im, K.S., Xie, X., et al.: Ultra-fast phase-contrast x-ray imaging of near-nozzle velocity field of high-speed diesel fuel sprays. In: ILASS Americas, 22nd Annual Conference on Liquid Atomization and Spray Systems, Cincinnati, Ohio, vol. 169 (2010)
16. Lin, K.C., Carter, C., Fezzaa, K., et al.: X-ray study of pure-and aerated-liquid jets in a quiescent environment. In: 47th AIAA Aerospace Sciences Meeting including The New Horizons Forum and Aerospace Exposition, Orlando, Florida, vol. 994 (2009)
17. MacPhee, A.G., Tate, M.W., Powell, C.F., et al.: X-ray imaging of shock waves generated by high-pressure fuel sprays. Science **295**(5558), 1261–1263 (2002)
18. Moon, S.: Novel insights into the dynamic structure of biodiesel and conventional fuel sprays from high-pressure diesel injectors. Energy **115**, 615–625 (2016)
19. Distler R., Hamann C., Krämer M., et al.: High speed X-ray imaging for nozzle exit velocity and density distribution measurements of GDI nozzles. In: ILASS Europe. 28th European Conference on Liquid Atomization and Spray Systems, Valencia, pp. 669–676 (2017)
20. Moon, S., Huang, W., Li, Z., et al.: End-of-injection fuel dribble of multi-hole diesel injector: comprehensive investigation of phenomenon and discussion on control strategy. Appl. Energy **179**, 7–16 (2016)
21. Li, Z.L., Zhao, W.B., Wu, Z.J., et al.: The measurement of internal surface characteristics of fuel nozzle orifices using the synchrotron X-ray micro CT technology. Sci. China Technol. Sci. **2018**, 1–7 (2018)
22. Matusik, K.E., Duke, D.J., Kastengren, A.L., et al.: High-resolution X-ray tomography of engine combustion network diesel injectors. Int. J. Engine Res. **19**(9), 963–976 (2018)
23. Bauer, D., Barthel, F., Hampel, U.: High-speed X-ray CT imaging of a strongly cavitating nozzle flow. J. Phys. Commun. **2**(7), 075009 (2018)
24. Duke, D.J., Swantek, A.B., Kastengren, A.L., et al.: X-ray diagnostics for cavitating nozzle flow. J. Phys. Conf. Ser. **656**(1), 012110 (2015)
25. Moon, S., Komada, K., Li Z., et al.: High-speed X-ray imaging of in-nozzle cavitation and emerging jet flow of multi-hole GDI injector under practical operating conditions. In: 13th Triennial International Conference on Liquid Atomization and Spray Systems, Tainan, Taiwan (2015)
26. Wang, F., He, Z., Liu, J., et al.: Diesel nozzle geometries on spray characteristics with a spray model coupled with nozzle cavitating flow. Int. J. Autom. Technol. **16**(4), 539–549 (2015)
27. Wang, B., Jiang, Y., Hutchins, P., et al.: Numerical analysis of deposit effect on nozzle flow and spray characteristics of GDI injectors. Appl. Energy **204**, 1215–1224 (2017)
28. Wu, Z., Li, Z., Gong, H., et al.: Comparisons of nozzle orifice processing methods using synchrotron X-ray micro-tomography. J. Zhejiang Univ. Sci. A **13**(3), 182–188 (2012)
29. Huang, W., Moon, S., Ohsawa, K.: Near-nozzle dynamics of diesel spray under varied needle lifts and its prediction using analytical model. Fuel **180**, 292–300 (2016)
30. Komada, K., Moon, S.: Transient needle motion of an outwardly opening GDI injector and its effects on initial spray formation. Fuel **181**, 964–972 (2016)
31. Als-Nielsen, J., McMorrow, D.: Elements of Modern X-ray Physics. Wiley, Hoboken (2011)
32. Li, Z., Wu, Z., Gao, Y., et al.: Development and application of an automatic measurement method for nozzle orifice diameter and length. J. Zhejiang Univ. Sci. A **16**(1), 11–17 (2015)
33. Huang, W., Gao, Y., Li, Z., et al.: Three-dimensional investigations of flow characteristics in a diesel nozzle. At. Sprays **23**(4), 343–361 (2013)
34. Li, Z., Wu, Z., Huang, W., et al.: Applications of synchrotron X-ray micro-tomography on nondestructive 3D studies of diesel nozzle internal micro-structure. J. Phys. Conf. Ser. **463**, 012045 (2013)

35. Huang, W., Wu, Z., Gong, H., et al.: Effect of nozzle geometry on macroscopic behavior of diesel spray in the near-nozzle field. SAE Technical Papers 2013-01-1587 (2013)
36. Huang, W., Moon, S., Gao, Y., et al.: Eccentric needle motion effect on near-nozzle dynamics of diesel spray. Fuel **206**, 409–419 (2017)
37. Gao, Y., Deng, J., Li, C., et al.: Experimental study of the spray characteristics of biodiesel based on inedible oil. Biotechnol. Adv. **27**(5), 616–624 (2009)
38. Zhang, X.S., Zhao, H., Hu, Z.J., et al.: Effect of biodiesel on the particle size distribution in the exhaust of common-rail diesel engine and the mechanism of nanoparticle formation. Sci. China Ser. E Technol. Sci. **52**(9), 2773–2778 (2009)
39. Wu, Z., Zhu, Z., Huang, Z.: An experimental study on the spray structure of oxygenated fuel using laser-based visualization and particle image velocimetry. Fuel **85**(10–11), 1458–1464 (2006)
40. Moon, S., Gao, Y., Park, S., et al.: Effect of the number and position of nozzle holes on in-and near-nozzle dynamic characteristics of diesel injection. Fuel **150**, 112–122 (2015)
41. Jeon, J., Moon, S.: Ambient density effects on initial flow breakup and droplet size distribution of hollow-cone sprays from outwardly-opening GDI injector. Fuel **211**, 572–581 (2018)